

# Diode-pumped Yb:GSO femtosecond laser

Wenxue Li, Qiang Hao, Hui Zhai, and Heping Zeng

Key Laboratory of Optical and Magnetic Resonance Spectroscopy, and Department of Physics, East China Normal University, Shanghai 200062, China  
[hpzeng@phy.ecnu.edu.cn](mailto:hpzeng@phy.ecnu.edu.cn)

Wei Lu

National Laboratory for Infrared Physics, Shanghai Institute of Technical Physics, Chinese Academy of Sciences, Shanghai 200083, China

Guangjun Zhao, Lihe Zheng, Liangbi Su, Jun Xu

Shanghai Institute of Optics and Fine Mechanics, Chinese Academy of Sciences, Shanghai 201800, China

**Abstract:** Compact femtosecond laser operation of Yb:Gd<sub>2</sub>SiO<sub>5</sub> (Yb:GSO) crystal was demonstrated under high-brightness diode-end-pumping. A semiconductor saturable absorption mirror was used to start passive mode-locking. Stable mode-locking could be realized near the emission bands around 1031, 1048, and 1088 nm, respectively. The mode-locked Yb:GSO laser could be tuned from one stable mode-locking band to another with adjustable pulse durations in the range 1~100 ps by slightly aligning laser cavity to allow laser oscillations at different central wavelengths. A pair of SF10 prisms was inserted into the laser cavity to compensate for the group velocity dispersion. The mode-locked pulses centered at 1031 nm were compressed to 343 fs under a typical operation situation with a maximum output power of 396 mW.

©2007 Optical Society of America

**OCIS codes:** (140.5680) Rare earth and transition metal solid-state lasers; (140.3480) Lasers, diode-pumped; (140.4050) Mode-locked lasers.

---

## References and links

1. F. Druon, S. Chénais, P. Raybaut, F. Balembois, P. Georges, R. Gaumé, G. Aka, B. Viana, S. Mohr, and D. Kopf, "Diode-pumped Yb:Sr<sub>3</sub>Y(BO<sub>3</sub>)<sub>3</sub> femtosecond laser," *Opt. Lett.* **27**, 197-199 (2002).
2. A. A. Lagatsky, A. R. Sarmani, C. T. A. Brown, W. Sibbett, V. E. Kisel, A. G. Selivanov, I. A. Denisov, A. E. Troshin, K. V. Yumashev, N. V. Kuleshov, V. N. Matrosov, T. A. Matrosova, and M. I. Kupchenko, "Yb<sup>3+</sup>-doped YVO<sub>4</sub> crystal for efficient Kerr-lens mode locking in solid-state lasers," *Opt. Lett.* **30**, 3234-3236 (2005).
3. E. Innerhofer, T. Sudmeyer, F. Brunner, R. Härring, A. Ashwanden, R. Paschotta, U. Keller, C. Hönninger, and M. Kumkar, "60-W average power in 810-fs pulses from a thin-disk Yb:YAG laser," *Opt. Lett.* **28**, 367-369 (2003).
4. F. Druon, S. Chénais, P. Raybaut, F. Balembois, P. Georges, R. Gaumé, P. H. Haumesser, B. Viana, D. Vivien, S. Dhellemmes, V. Ortiz, and C. Larat, "Apatite-structure crystal, Yb<sup>3+</sup>:SrY<sub>4</sub>(SiO<sub>4</sub>)<sub>3</sub>O, for the development of diode-pumped femtosecond lasers," *Opt. Lett.* **27**, 1914-1916 (2002).
5. F. Thibault, D. Pelenc, F. Druon, Y. Zaouter, M. Jacquemet, and P. Georges, "Efficient diode-pumped Yb<sup>3+</sup>:Y<sub>2</sub>SiO<sub>5</sub> and Yb<sup>3+</sup>:Lu<sub>2</sub>SiO<sub>5</sub> high-power femtosecond laser operation" *Opt. Lett.* **31**, 1555-1557 (2006).
6. A. Lucca, G. Debourg, M. Jacquemet, F. Druon, F. Balembois, P. Georges, P. Camy, J. L. Doualan, and R. Moncorgé, "High power diode-pumped Yb<sup>3+</sup>:CaF<sub>2</sub> femtosecond laser," *Opt. Lett.* **29**, 2767-2769 (2004).
7. Y. Zaouter, J. Didierjean, F. Balembois, G. L. Leclin, F. Druon, P. Georges, J. Petit, P. Goldner, and B. Viana "47-fs diode-pumped Yb<sup>3+</sup>:CaGdAlO<sub>4</sub> laser," *Opt. Lett.* **31**, 119-121 (2006).
8. V. E. Kisel, A. E. Troshin, V. G. Shcherbitsky, N. V. Kuleshov, V. N. Matrosov, T. A. Matrosova, M. I. Kupchenko, F. Brunner, R. Paschotta, F. Morier-Genoud, and U. Keller, "Femtosecond pulse generation with a diode-pumped Yb<sup>3+</sup>:YVO<sub>4</sub> laser" *Opt. Lett.* **30**, 1150-1152 (2005).

9. M. Jacquemet, C. Jacquemet, N. Janel, F. druon, F. Balembos, P. Georges, J. Petit, B. Viana, D. Vivien, B. Ferrand, "Efficient laser action of Yb:LSO and Yb:YSO oxyorthosilicates crystals under high-power diode-pumping," *Appl. Phys. B* **80**, 171-176 (2005).
10. W. Li, H. Pan, L. Ding, H. Zeng, G. Zhao, C. Yan, L. Su, and J. Xu, "Efficient diode-pumped Yb:Gd<sub>2</sub>SiO<sub>5</sub> laser", *Appl. Phys. Lett.* **88**, 221117 (2006).
11. S. Chénais, F. Druon, F. Balembos, G. Lucas-Leclin, P. Georges, A. Brun, M. Zavelani-Rossi, F. Augé, J.-P. Chambaret, G. Aka, D. Vivien, "Multiwatt, tunable, diode-pumped CW Yb:GdCOB laser," *Appl. Phys. B* **72**, 389-393 (2001).
12. W. Li, H. Pan, L. Ding, H. Zeng, G. Zhao, C. Yan, L. Su and J. Xu, "Diode-pumped continuous-wave and passively mode-locked Yb:GSO laser", *Opt. Express* **14**, 686-685 (2006).

## 1. Introduction

Ytterbium-doped crystals that typically have broad emission bands around 1  $\mu\text{m}$  have been recognized in recent years as very attractive gain media for diode-pumped femtosecond (fs) oscillation and amplification [1-8]. Ytterbium ion has a very simple electronic-level scheme involving only two manifolds  $^2F_{5/2}$  and  $^2F_{7/2}$ , which consequently eliminates undesired effects such as excited-state absorption, cross relaxation, up-conversion, and concentration quenching. Its relatively low intrinsic quantum defects (generally less than 10%) and high radiative quantum efficiency results in a low heat generation that may support efficient and compact diode-pumped lasers. An important advantage of Yb-doped laser crystals over their Nd-doped counterparts is their broad emission spectra, which allows ultrashort pulse generation. Many Yb-doped materials have been already demonstrated as competitive laser gain media in the fs regime [1-8]. Among these new materials, Yb-doped glasses exhibit very broad and smooth emission spectra that permit possible generation of ultrashort pulses, but poor thermal conductivity and low stress-fracture which limit their applications in high-power laser systems. High-power compact lasers make use of Yb-doped crystals with comparatively high thermal conductivities and large emission cross-sections. Nevertheless, Yb<sup>3+</sup> ions in crystalline host matrices typically have narrow emission and absorption bands. The splittings of the fundamental manifold  $^2F_{7/2}$  of Yb<sup>3+</sup> in most of the Yb-doped crystals are only a few hundreds of  $\text{cm}^{-1}$ , comparable to the thermal energy at room temperature, which may cause strong re-absorption at the emission wavelengths due to thermal populating of the terminal laser level. These problems have been partly solved in some recently developed ytterbium-doped oxyorthosilicates, such as Yb:Y<sub>2</sub>SiO<sub>5</sub> (Yb:YSO), Yb:Lu<sub>2</sub>SiO<sub>5</sub> (Yb:LSO), and Yb:GSO, which have been demonstrated to exhibit broad emission spectra, large ground-state splittings, and high thermal conductivities [9,10]. High-power fs laser oscillations of Yb:YSO and Yb:LSO have already been demonstrated [5]. Yb:GSO has been demonstrated to exhibit a large fundamental manifold splitting up to 1067  $\text{cm}^{-1}$ , and a broad emission bandwidth in the range 1020-1120 nm with a full-width of half maximum of 77 nm, which supports broadband tunable cw or ultrafast lasers. Tunable cw Yb:GSO lasers have been realized efficiently with low LD pump thresholds [10]. In this letter we report on fs operation of Yb:GSO laser.

A large manifold splitting of Yb<sup>3+</sup> ions in the GSO host indicates a quite strong crystal-field interaction notably due to the anisotropic and compact structure of the GSO oxyorthosilicate host matrix. The crystal structure of the GSO belongs to the primitive monoclinic space group P2<sub>1</sub>/c and is composed of a two-dimensional network of corner linked (OGd<sub>4</sub>) tetrahedra where the (SiO<sub>4</sub>) tetrahedra are packed. In comparison, the structures of YSO and LSO belong to the end-centered monoclinic I2/a space group, where (SiO<sub>4</sub>) and (OY<sub>4</sub>) or (OLu<sub>4</sub>) tetrahedra share edges and form chains interconnected by isolated (SiO<sub>4</sub>) tetrahedra. Accordingly, the GSO is more anisotropic and has more compact structure than YSO or LSO, which results in a larger manifold splitting for Yb<sup>3+</sup>. In the GSO host lattice, there are two nonequivalent crystallographic sites of Gd<sup>3+</sup>, site Gd<sub>1</sub> and Gd<sub>2</sub>, which are coordinated with 7 and 9 oxygen atoms, respectively. Accordingly, there exist two substitution sites for ytterbium-doping. In site Gd<sub>1</sub>, the Yb<sup>3+</sup> ion is affected by the stronger crystal-field and results in a larger Stark-splitting of the Yb<sup>3+</sup> manifolds.

## 2. Spectral properties of Yb:GSO

In the previous work, we measured room-temperature absorption and emission spectra of a thick Yb:GSO sample [10]. A strong re-absorption loss was observed near the zero-phonon emission line, which corresponds to the absorption maximum at 976 nm. To confirm that the abnormal emission around the zero-phonon line are caused by the strong re-absorption in thick samples, we re-examined the emission spectrum of a 0.82-mm-thick 5at% Yb-doped sample with a Triax550 spectrofluorimeter under the 940 nm laser diode excitation. The absorption and emission spectra are presented in Fig.1. As expected, a clear emission peak appears at the 976 nm, with a cross section of  $0.24 \times 10^{-20} \text{ cm}^2$ . The emission cross section at 1088 nm was determined to be  $0.44 \times 10^{-20} \text{ cm}^2$ , nearly equal to the value of the 9.48-mm-thick sample [10]. The absorption band around 976 nm overlaps with the shortest-wavelength emission band, corresponding to the zero-line transition between the lowest levels of  $^2F_{7/2}$  and  $^2F_{5/2}$  manifolds. The emission bands centered around 1013, 1031, 1048, and 1088 nm correspond to transitions from the ground state  $^2F_{7/2}$  to the other sublevels of  $^2F_{5/2}$ , respectively. The emission band at the longest wavelength around 1088 nm corresponds to the transition from the lowest levels of the  $^2F_{5/2}$  manifold to the highest levels of the  $^2F_{7/2}$  manifold, which also has the largest cross section. We can therefore estimate the maximum splitting of the  $^2F_{7/2}$  manifold as  $1067 \text{ cm}^{-1}$ , which is much larger than those in Yb:YSO and Yb:LSO, and even  $1003 \text{ cm}^{-1}$  splitting in Yb:GdCOB [11]. Such a large fundamental splitting helps to reduce thermal population of the terminal laser level and thus to decrease the laser threshold. This should in principle benefit mode-locking around the broadband emission bands.

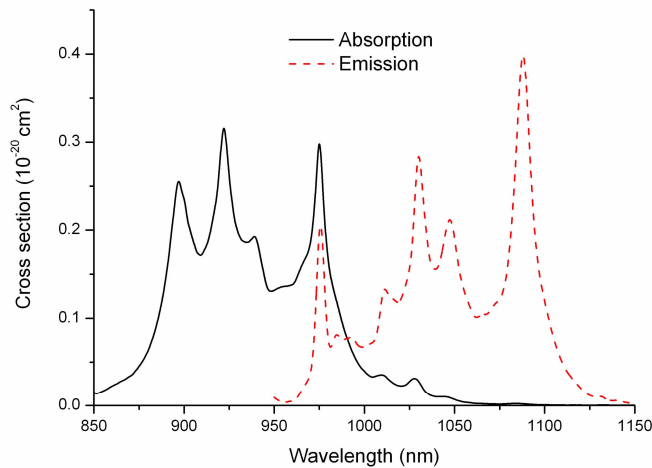


Fig. 1. Room-temperature absorption and emission spectra of a 0.82-mm-thick 5at% Yb:GSO.

## 3. Experimental setup

In this paper, we report on fs pulse generation in a compact Yb:GSO laser under direct high-brightness laser diode pumping, where passive mode-locking is started with a semiconductor saturable-absorber mirror (SESAM). In comparison with the so-called Kerr-lens mode-locking technique commonly used in ultrafast lasers, SESAM-based mode-locking offers advantages such as release of critical requirements of precise cavity design and alignment, and ease in self-starting mode-locking. It is especially applicable to laser oscillators that are inappropriate to operate Kerr-lens mode-locking, such as the mode-locked operation of Yb lasers that typically exhibit low stabilities intrinsically related with the long excited-state lifetimes of  $\text{Yb}^{3+}$  ions. Recently, we have generated picosecond pulses from SESAM-based passive mode-locking in a Yb:GSO laser end-pumped by a fiber-coupled laser diode with the

fiber core diameter of 400  $\mu\text{m}$  [12]. It is well-known that the strong tendency toward Q-switched mode-locking of Yb lasers can be suppressed by choosing a proper intracavity beam diameter on the SESAM and optimizing the pump arrangement to get a small mode area in the gain medium. For this purpose, we employed a high-brightness laser diode with a fiber core diameter and numerical aperture of 50  $\mu\text{m}$  and 0.22, respectively. The laser cavity loss was minimized to reach high intracavity pulse energies.

In order to generate stable fs pulses from a compact Yb:GSO laser, we employed a folded resonator as schematically shown in Fig. 2. The laser resonator consists of a SESAM and four mirrors: an input flat mirror  $M_1$  with high transmission at 974 nm and high reflection in a broad band from 1020 to 1120 nm, two folded concave mirrors  $M_2$  ( $R=500$  mm) and  $M_3$  ( $ROC=300$  mm) both with high reflection in a broad band from 1020 to 1120 nm, and an output coupler (OC) flat mirror with a transmission of 2.5%. The length between  $M_1$  and  $M_2$  is about 295 mm, while  $M_2$  and OC are separated by 360 mm, and the length between OC and SESAM is 826 mm. The total cavity length is 1481 mm. Our SESAM is a commercially available one (BATOP GmbH, Germany), which has a 2% saturable absorption at 1064 nm, 70- $\mu\text{J}/\text{cm}^2$  saturation fluence, and 20-ps relaxation time constant. The experiment was performed with a 2-mm-long 5%-doped Yb:GSO crystal, which was antireflection-coated at 974 nm and a broad band from 1020 to 1120 nm. To efficiently remove the generated heat under diode-pumping, we wrapped the crystal with indium foil and fixed it tightly in a water-cooled copper heat sink. The temperature of the laser crystal was controlled at 14°C. The high-brightness fiber-coupled laser diode used for end-pumping was controlled by a temperature regulation to emit at 974 nm with the maximum power up to 5 W.

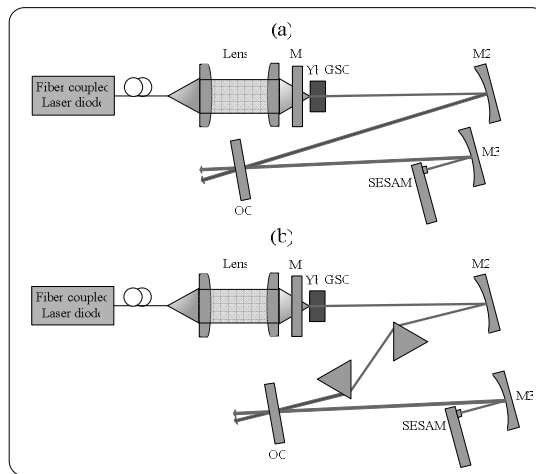


Fig. 2. Experimental setup for cw mode-locked Yb:GSO laser (a), and that with intracavity SF10 prisms for pulse compression (b).

The laser cavity was carefully designed to guarantee a sufficient small mode area in the gain medium and appropriate operation of SESAM in the strong saturation regime within its damage threshold. With the folded cavity as shown in Fig. 2, we can estimate by the so-called ABCD analysis that the beam waists were near 58  $\mu\text{m}$  on the SESAM and 50  $\mu\text{m}$  in the crystal, respectively. By using the setup of Fig. 2(a) with a 2.5% output coupler, the Yb:GSO laser was operated in the picosecond regime at a repetition rate of 101 MHz with the transverse mode remained as  $\text{TEM}_{00}$ . The mode-locked pulse train was detected by a fast photodiode with a rising time of less than 200 ps and recorded with a digital storage oscilloscope. The standard deviations of the cw mode-locked Yb:GSO laser pulses are shown in Fig. 3 along with the pulse power spectrum recorded by a spectral analyzer (Agilent E4411B), which clearly show that the cw mode-locked laser was stably operated at 101 MHz

without any observable sidebands. The shot-to-shot fluctuation and long-term mode-locking stability were monitored by checking the output pulse energy. In comparison with the case under high-power pumping with fiber-coupled LD of a large fiber-core diameter, a small mode area in the gain medium made the cw mode-locking to start up more easily and to operate more stably.

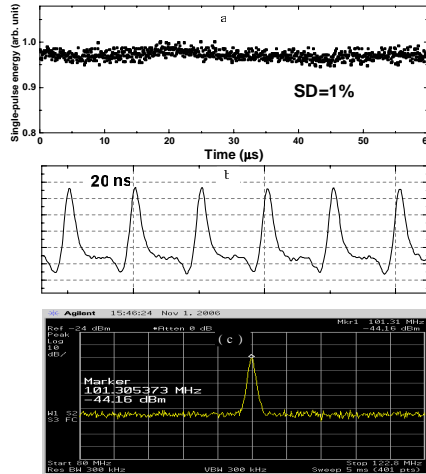


Fig. 3. (a) The standard deviations of the cw mode-locked Yb:GSO laser pulses. (b) The 101 MHz repetition rate of the cw mode-locked pulses. (c) Power spectrum of a cw mode-locked Yb:GSO laser.

#### 4. Results and discussions

In the absence of intra-cavity prisms for pulse compression, the output pulses reached 1.3 ps at 1031 nm with a maximum average output power of 586 mW. As shown in Fig. 4(a), the measured autocorrelation traces are well-fitted assuming a  $\text{sech}^2$  pulse shape. The output spectrum was recorded with a fiber-based spectrometer. As typically presented in the inset of Fig. 4(b), the 1031 nm pulse have a full-width of half-maximum (FWHM) of 4.2 nm. According to the emission spectrum of Yb:GSO, laser action may occur around the strong emission bands of 1013, 1031, 1048, and 1088 nm. Laser emissions around 1013 nm suffer from strong reabsorption losses caused by thermal populating of the terminal laser level. The intermediate bands around 1031 and 1050 nm have medium emission cross-sections where the terminal levels are a little populated. Efficient laser actions are possible. The band around 1088 nm has the strongest emission cross-section with the corresponding terminal laser level very few populated with a probability of  $6 \times 10^{-3}$  at room temperature according to the Boltzman thermal distribution. As a result, Yb:GSO laser at 1088 nm nearly approaches a quasi-four-level laser scheme, which results in an easy population inversion and a low pump threshold. Depending on the substitution sites, ytterbium ions in Yb:GSO exhibit different but large overall splittings of the ground-state manifold  $^2F_{7/2}$ . Nevertheless, ytterbium ions in the GSO host matrix have separate emission bands, corresponding to transitions from the lowest levels of  $^2F_{5/2}$  manifold to the split levels of  $^2F_{7/2}$  manifold. Separate terminal laser sub-levels limit the continuously tunable range of the cw laser operation. Without any intracavity wavelength selectors, the quasi-four-level nature results in a cw laser oscillation at long wavelengths depending on the laser crystal length and the OC transmission. While in the mode-locked laser operation, the preferred lasing wavelengths differ from that of the cw laser operation. Stable mode-locking could be realized near the emission bands around 1031, 1048, and 1088 nm, respectively. Near the emission valleys between two adjacent emission bands,

mode-locking was unstable, and multi-wavelength hops were observed as the laser cavity was intentionally aligned for lasing at the valley emission wavelengths. This limited the achievable broadband laser spectra. In the stable mode-locked band near 1088 nm, long pulse durations were observed. For instance, the mode-locked pulse centered at 1092 nm, under the typical operation with a maximum average output power of 602 mW by using a 2.5% output coupler, had a pulse duration of 103 ps (assuming a  $\text{sech}^2$  pulse shape). This could be ascribed to the fact that the SESAM used in the experiment, whose saturation absorption centered around  $1064 \pm 5$  nm, had a smaller saturation fluence around longer central wavelengths. It is well known that a smaller modulation depth typically leads to longer pulses. In addition, the dispersion of the gain medium may differ under different emission bands due to the corresponding electronic resonances between the lowest levels of  $^2F_{5/2}$  manifold and the split levels of  $^2F_{7/2}$  manifold as separate terminal laser sub-levels. As the central wavelength of the mode-locked Yb:GSO laser could jump from one stable mode-locking band to another by slightly adjusting the laser cavity, mode-locked pulse duration could be correspondingly adjustable in the range 1~100 ps by slightly aligning laser cavity to allow laser oscillations at different wavelengths. Wavelength tuning was mainly determined by the reabsorption loss in the gain medium and spatial mode-matching between the pump and intracavity laser.

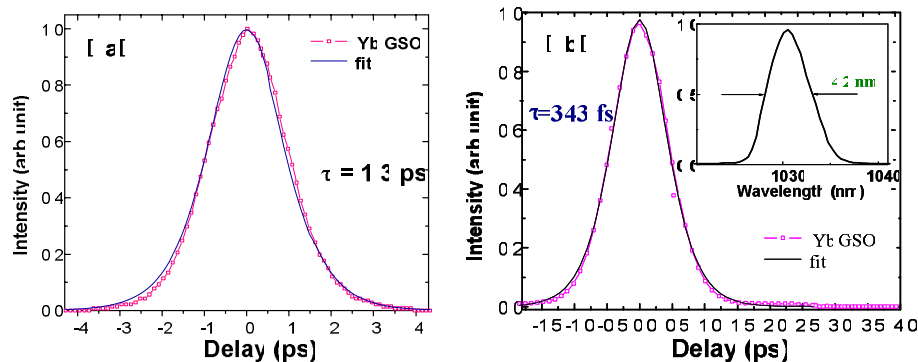


Fig. 4. Autocorrelation trace of the cw mode-locked Yb:GSO laser (a) and that with intracavity SF10 prisms for pulse compression (b). The inset of (b) gives the corresponding spectrum of the 343 fs pulse.

## 5. Conclusions

In conclusion, we have demonstrated what we believe is the first diode-pumped fs Yb:GSO laser. This oxythosilicate crystal has the unique property of high structural disorder and thus exhibits a very broad emission band of 77 nm. The demonstrated maximum output power of 396 mW is not a limit. Further progress could be expected by improving Yb-doped GSO crystal homogeneity and purity, which may enable a high doping concentration and thus more powerful laser concepts. Driven by these demonstrated promising advantages, high-quality Yb:GSO laser crystals are competitive alternatives to the widely-used Ti:sapphire crystals as compact, tunable fs solid-state lasers operated in the 1  $\mu\text{m}$  wavelength regime.

## Acknowledgments

This work was partly supported by National Natural Science Fund (Grant No. 10525416, 10374028 and 60478011), National key project for basic research (Grant No. 2006CB806000 and 2004CB619004), Key Projects from Science and Technology Commission of Shanghai Municipality (Grant No. 04dz14001, 06SR07102, and 06JC14025), and Program for Changjiang Scholars and Innovative Research Team (PCSIRT).